

# Solid-State Backscattered-Electron Detector for Sub-keV Imaging in Scanning Electron Microscopy

A. Šakić, L. K. Nanver, G. van Veen, K. Kooijman, P. Vogelsang, T. L. M. Scholtes, W. de Boer, W. Wien, S. Milosavljević, C. Th. H. Heerkens, T. Knežević, I. Spee

**Abstract**— The low-energy electron detectors presented in this work have near theoretical electron signal gain at low energies measured down to 200 eV and high-speed response due to the following technological steps: (i) chemical vapor deposition (CVD) of boron layers (PureB layers) proven to form an ideal nm-deep p<sup>+</sup>n junction with the outstanding sensitivity to low-energy electrons [1], and (ii) defect-free, ultra-low doped, 40 μm thick n<sup>-</sup> epitaxial layer which facilitates capacitance values as low as 3 pF/mm<sup>2</sup>. The fabricated detectors have been placed in SEMs and the resulting high-resolution images, robustness to the electron irradiation, and high scanning speeds make them promising candidates for the future solid-state backscattered-electron (BSE) detectors.

**Index Terms**— Pure boron depositions, electron detection, low-energy electrons, backscattered electrons, high efficiency detection, SEM detectors

## I. INTRODUCTION

Low-voltage Scanning Electron Microscopy (SEM) is becoming the preferred tool for nanometer-scale inspection in the semiconductor industry. It provides an atomic-scale resolution of a specimen surface due to short range of the electrons in matter, and suppression of effects such as charging of insulating materials, heating, and damage of the sample. However, the detection of sub-keV electron beams demands special detector strategies that can detect low-penetration radiations. Several demonstrations of such radiation detectors are given in [1-3] comprising the photodiodes based on a recently developed boron layer technology (PureB technology) for creating nm-deep p<sup>+</sup>n junctions that have been proven to give exceptionally high responsivity for low-penetration-depth radiation such as deep/extreme ultra-violet light (DUV/EUV)

Agata Šakić, Lis K. Nanver, Tom L. M. Scholtes, W. de Boer, W. Wien, and S. Milosavljević are with the Laboratory of Electronic Components, Technology and Materials (ECTM), Delft Institute of Microsystems and Nanoelectronics (DIMES), Delft University of Technology, Feldmannweg 17, 2628 CT Delft, The Netherlands (phone: +31 (0)15 2782185, fax: +31 (0)15 2622163, email: a.sakic@tudelft.nl)

Carel Th. H. Heerkens is with the Charged Particle Optics, Imaging Science and Technology, Applied Sciences, Delft University of Technology

Gerard van Veen, Kees Kooijman, Patrick Vogelsang, and I. Spee are with the FEI Company, The Netherlands

T. Knezevic is with the ZEMRIS, FER, University of Zagreb, Croatia

and low energy electrons. PureB photodiodes are used in this paper as building blocks for electron detectors that will be tested in flexible configurations to obtain optimized topographical and/or compositional contrast imaging. Additionally, the effect of electron beam irradiation on the PureB pn-junction is evaluated.

The imaging speed of the detector is determined by a detector bandwidth (RC constant) where the dominating parameter is the junction capacitance of a photodiode. High resistivity substrates that provide sufficiently low doping to obtain the low capacitance values result in high parasitic resistances. Therefore, ultra-low doped epitaxial layers are grown on n-type 2-5 Ωcm Si (100) substrates. In this way, the resistance values are predetermined by the wafer selection and the capacitance value is tuned with the epi-layer thickness. In the present work, up to 40-μm-thick high-quality defect-free epi-layers are grown in a commercial Si/SiGe chemical-vapor-deposition (CVD) epitaxial reactor system. For achieving the light doping levels of  $<10^{12}$  cm<sup>-3</sup> that are dictated by the strict capacitance specifications, the growth conditions and the starting doping level will be described.

The placement of the detector in an SEM system requires a through-wafer aperture etched close to the innermost diodes of the detector, as shown in Fig. 1. After the bulk-micromachining, the detectors are finally placed in SEM systems and high resolution images are acquired.

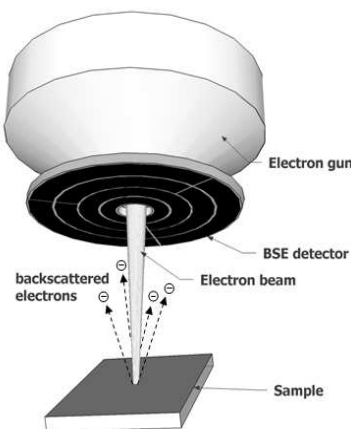


Fig. 1. Conceptual drawing of a SEM system showing the location of the annular BSE detector.

## II. B-LAYER PHOTODIODES

A  $p^+n$  junction is formed by CVD of a diborane ( $B_2H_6$ ) at 700 °C in an epitaxial reactor. The boron adsorbs on silicon in an amorphous phase (PureB), part of which reacts with silicon surface (Fig. 2a). The limited diffusion of dopants at 700 °C and high gas source flow rate provide ultrashallow and highly-doped junctions (Fig. 2b). In order to capture the nm-deep-penetrating sub-keV electrons in silicon, the pn-junction has to be as shallow as possible. The minimum thickness that guarantees a uniform boron deposition is around 2 nm where the ideal I-V characteristics and the small over-the-wafer spread of the dark current indicate a reliable process [4]. To measure the sensitivity of the as-deposited layer, the photodiode has been subjected to the electron beam of a SEM system. The reference value is measured in a Faraday cup mounted with the photodiode and the resulting ratio between the photodiode current  $I_{ph}$  and the Faraday cup current  $I_F$  gives the electron signal gain of the diode. As seen in Fig. 3, they have superior performance as compared to commercially available BSE detectors and “low Voltage high Contrast Detectors” (vCDs), as reported in [3]. At the lowest measured energy of 500 eV for the commercial BSE detector, more than a factor 5 improvement in sensitivity is obtained with the PureB diodes. Further measurement down to 200 eV yielded a record-high electron gain of 33 is achieved.

The electrical stability of the PureB photodiodes is tested during the electron irradiation. The values of the dark current are recorded before and after the electron exposure. A series of exposures were performed with variable exposure energy, spot size, and exposed region on the detector. The increase of dark current, i.e. dark current degradation has been observed only in cases when the diode edge is exposed. The exposure of the edge means that the electron beam is exposing the PureB layer as well as the perimeter of the diode where PureB borders with the insulating oxide and metallization layers. The increase in dark current could be explained by the commonly observed effect that irradiation can disrupt hydrogen-bonds that are intentionally formed during alloying to reduce the oxide/silicon interface trap density. It is well-known that these H-bonds can be restored by thermal annealing even at very low temperatures. As shown in Fig. 4, after performing 1h bake

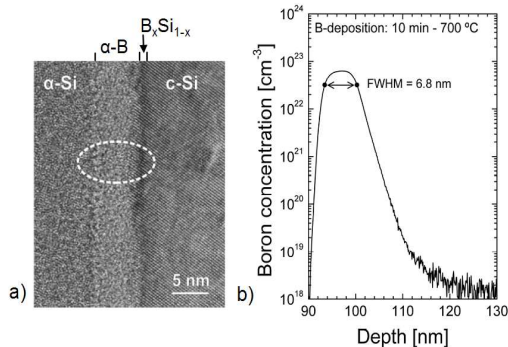


Fig. 2. (a) High-resolution TEM image and (b) SIMS profile ( $O_2^+$  primary ion beam at 1 keV) of an as-deposited B-layer formed on a (100) Si surface at 700 °C after 10 min  $B_2H_6$  exposure (1).

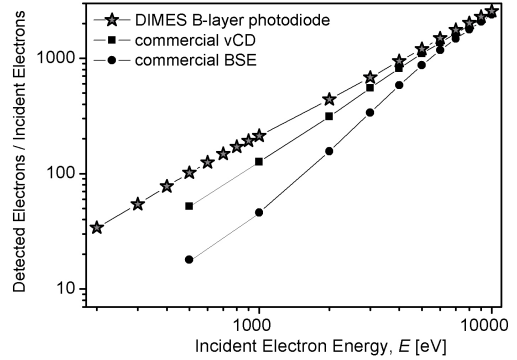


Fig. 3. Measured electron signal gain for a DIMES B-layer photodiode, a commercially available BSE detector and a low Voltage high Contrast Detector (vCD).

step at 200 °C, the current has restored to the initial value. It can therefore be concluded that dark current degradation is related to perimeter oxide-related effects that can be readily recovered with the baking step, or in time. In accordance with these results, also no optical degradation was observed during any of the optical testing.

With the ultrashallow junction responsivity benefits, and the degradation robustness, the described PureB layers have several other advantages that are vital for the final detector performance. First, the PureB layer is a diffusion barrier for pure aluminum. Namely, pure Al is commonly avoided in combination with silicon due to the “spiking” nature of the contact. In this case however nm-thin PureB layer prevents the spiking and allows the pure Al to be deposited directly on the photosensitive surface [5]. This solves a problem of a conventional Al/Si (1%) alloy that would leave Si precipitates on surface when metallization layer is selectively etched from the PureB layer. As described in [4], the smallest metallization residues on the responsive surface will degrade the efficiency performance. Second, diluted HF (0.55%) is highly selective to the boron layers, but it etches pure Al. Therefore, the process is simplified and carried out without the etch-stop layers in forming metal contacts or a surface protection layers. It also enables patterning of the metal contacts, e.g. conductive grid to reduce the series resistance of a photodiode.

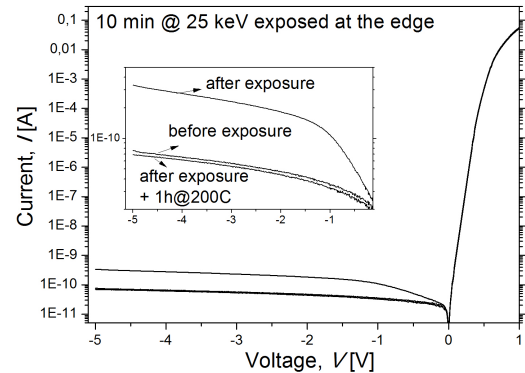


Fig. 4. The I-V characteristics of a photodiode before and after a 10-min electron-irradiation at 25 keV when exposed at the edge of the device with the additional 200 °C thermal annealing step (below).

### III. SEGMENTATION AND LOW CAPACITANCE

Modern solid-state detectors demand flexible multi-segmentation (pixelization) of the photosensitive surface with closely-packed segments, example of which is shown in Fig. 5. This implies that the depletion region of every diode that builds the detector has to be vertically wide to obtain the low capacitance and series resistance, but laterally limited in order for neighboring detector segments (adjacent diodes) to function independently if application demands. One solution is to fabricate detectors on high resistivity, high-quality, thick epitaxial layers, grown on low-to-medium resistivity substrates, thus providing wide depletion, lateral isolation, and low series resistance through the substrate.

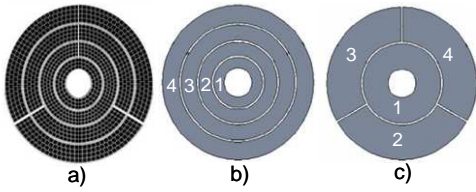


Fig. 5. (a) The electron detector consists of eight segments that can be used in two modes by combining the signal of segments into the (b) CBS - Concentric-Back-Scattered and (c) ABS - Angular-Back-Scatter mode.

Here the well-controlled lightly doped epitaxial  $n^-$ -layer is grown by auto-doping from the beforehand grown 300-nm-thick As doped epi layer. The final thickness of the epi-layer is set to 40  $\mu\text{m}$ . The growth of the As doping-source layer defines the As surface doping prior to the epi-layer growth and the background doping level of the chamber, which makes it decisive for the final doping of the lightly-doped epi. In this work we tested the As seed layers with  $10^{16}$  and  $10^{17} \text{ cm}^{-3}$  doping levels. It can be seen in Fig. 6 that when the  $10^{17} \text{ cm}^{-3}$  starting doping is applied, it will result in the level higher final doping incorporated in the 40- $\mu\text{m}$ -thick epi-layer when compared to the case of  $10^{16} \text{ cm}^{-3}$  starting level. Higher doping values will negatively reflect to the capacitance values, thus  $10^{16} \text{ cm}^{-3}$  starting level is favored for the detector fabrication. The C-V doping profile of a 40- $\mu\text{m}$ -thick epi-layer with the  $10^{16} \text{ cm}^{-3}$  seed layer places the doping level in the targeted sub- $10^{12} \text{ cm}^{-3}$  range. The full depletion of the layer is then reached already around 5 V. This is vital to reduce the parasitic resistance influence from the low-doped epi-layer region that

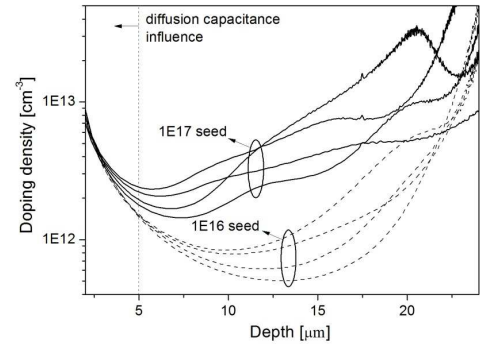


Fig. 6. C-V doping profiles of a 40- $\mu\text{m}$ -thick  $n^-$  epitaxial layer showing the doping density and the corresponding voltages.

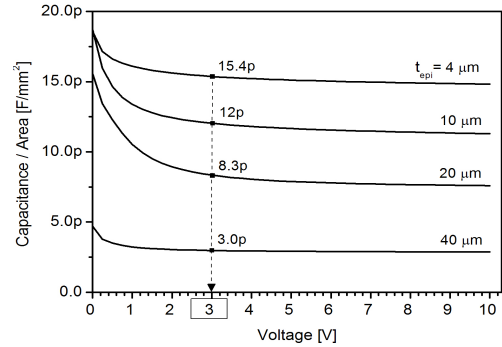


Fig. 7. Capacitance-voltage measurements of B-layer photodiodes for epitaxial layer thicknesses of 4  $\mu\text{m}$ , 10  $\mu\text{m}$ , 20  $\mu\text{m}$ , and 40  $\mu\text{m}$ .

contributes to the total series resistance if undepleted.

Various epi-layer thicknesses were fabricated as well and, as seen in Fig. 7, capacitances as low as 3 pF/ $\text{mm}^2$  are obtained for a 40  $\mu\text{m}$  thick layer at 3 V reverse bias. For the layer thicknesses of 4, 10, and 20  $\mu\text{m}$  the capacitance values are respectively 15.4, 12, and 8.3 pF/ $\text{mm}^2$ .

The 40- $\mu\text{m}$ -thick epi-layer is used as a substrate for the PureB detector. The detector diodes are kept 100  $\mu\text{m}$  apart, divided by the  $n^+$ -channel stop layer that help limit the lateral depletion spread, as shown in Fig. 8. The detector consists of 8 diodes as shown in Fig. 5, that can be further combined in different configurations. As a demonstration, the CBS configuration mode of the PureB detector showed in Fig. 5b is used to image an uncoated pollen sample at 50 eV (Fig. 9). The sharpest signals of the two inner concentric circles are combined in the inset to give the optimal image contrast.

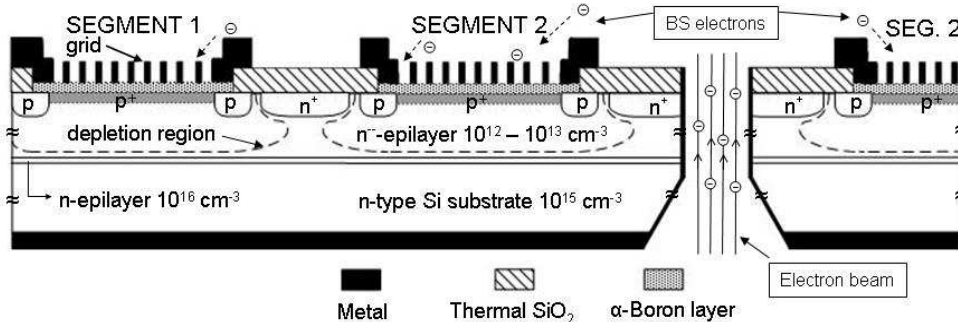


Fig. 8. Schematic cross-section of two neighboring segments of a PureB-layer detector with a through-wafer hole as aperture for the electron beam. The depletion of the typically 40  $\mu\text{m}$  deep  $n^-$  epitaxial layer is indicated. Segments are isolated by the  $n^+$ -channel-stop and the undepleted  $n^-$  layer.

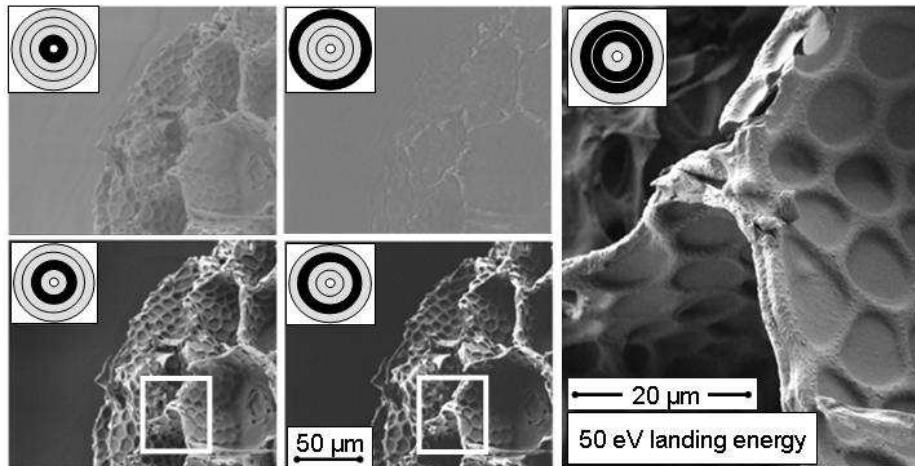


Fig. 9. Imaging of uncoated pollen sample at 50V landing energy for (a) each segment in CBS mode and (b) the optimal combination of segments. The insets indicate the operating segments.

#### IV. GRID PROCESSING FOR LOW RESISTANCE

The  $p^+$  anode and  $\alpha$ -B layers together have a sheet resistance of  $\sim 10$  k $\Omega$ . To nevertheless obtain a low series resistance on large diode segments, an Al grid is patterned directly on the diode surface. This is possible because the Al makes good ohmic contact to the PureB layer and it can be selectively removed by etching in HF, as mentioned in the previous sections. In this way the metal tracks to the segments, an Al perimeter contact to the diode, and the grid can be formed in one and the same Al layer as shown in Fig 10. With 1  $\mu\text{m}$  grid dimensions that frame squares of  $200 \times 200 \mu\text{m}^2$  as illustrated in Fig. 10, a less than 2% Al coverage of the front-window is feasible and therefore does not degrade the detection efficiency performance, yet it considerably lowers the diode resistance. For example, such grid lowers the series resistance from 280  $\Omega$  to 20  $\Omega$  for a 44  $\text{mm}^2$  large diode.

#### V. CONCLUSIONS

The new silicon-photodiode electron-detector technology demonstrates an impressive enhancement of the performance of SEM systems. In terms of electron signal gain, PureB detectors outperform the state-of-art backscattered-electron detectors by a factor 5 at 500 eV.

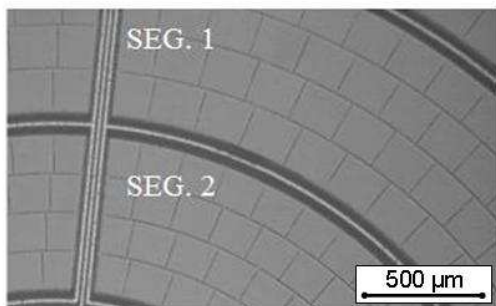


Fig. 10. Example of a conductive grid of Al on the photosensitive surface of the detector.

Furthermore, the overall electron signal gain in sub-keV range exhibits unprecedented performance as compared to both research and commercial detectors [3]. The fabrication technology is highly reliable and enables flexible configurations including segmented, closely-packed photodiodes and through-wafer apertures. The detectors are fabricated on a thick well-controlled lightly-doped epitaxial layer, with which capacitance values as low as 3 pF/ $\text{mm}^2$  were realized. High scanning speeds are additionally secured by patterning an Al grid on the photosensitive surface to also keep the series resistance low. An 8-segment back-scattered electron detector was fabricated and the measurement results demonstrate the versatility of this detector technology in obtaining optimal images even for landing energies as low as 50 eV.

#### ACKNOWLEDGMENTS

The authors would like to thank the staff of the DIMES ICP cleanrooms and measurement room for their support in the fabrication and measurement of the experimental material. The support of FEI Company is gratefully acknowledged for the help with the detector implementation and SEM imaging. This work has also received financial support from the Nuffic Huygens Scholarship Programma and has profited from cooperation with the SmartMix MEMPHIS Project and the STW Thin Film Nanomanufacturing Program.

#### References

- [1] F. Sarubbi, T.L.M. Scholtes, and L. K. Nanver, in *Journal of Electron. Material*, vol. 39, no. 2, pp. 162-173, 2010.
- [2] L. Shi, S. Nihtianov, L.K. Nanver, U. Kroth, A. Sakic, and A. Gottwald, *Proceedings of IEEE Sensors 2010*, pp. 132-135
- [3] A. Sakic, L. K. Nanver, G. van Veen, K. Kooijman, P. Vogelsang, T. L. M. Scholtes, W. de Boer, W. H. A. Wien, S. Milosavljevic, C. Th. H. Heerkens, T. Knežević, I. Spee, *IEDM 2010, IEDM10-712 P.31.4.1-31.4.4*
- [4] A. Šakić, Lis K. Nanver, T. L. M. Scholtes, C. Th. H. Heerkens, G. van Veen, K. Kooijman, and P. Vogelsang, *ESSDERC 2010*, pp. 102-105
- [5] A. Sakic, G. Lorito, F. Sarubbi, T. L. M. Scholtes, J. van der Cingel, L. K. Nanver, *Proc. of SAFE 2009*, pp. 112-115